Membrane microdomains modulate oligomeric ABCA1 function: impact on apoAI-mediated lipid removal and phosphatidylcholine biosynthesis[S]

Iulia Iatan,*,[1] Dana Bailey,*,[1] Isabelle Ruel,[†] Anouar Hafiane,[†] Steven Campbell,* Larbi Krimbou,[†] and Jacques Genest[†,2]

Department of Biochemistry* and Division of Cardiology,[†] Faculty of Medicine, McGill University Health Center/Royal Victoria Hospital, Montréal, Québec, H3A 1A1, Canada

Abstract **Recent studies have identified an ABCA1-dependent, phosphatidylcholine-rich microdomain, called the "high-capacity binding site" (HCBS), that binds apoA-I and plays a pivotal role in apoA-I lipidation. Here, using sucrose gradient fractionation, we obtained evidence that both ABCA1 and [^{125}I]apoA-I associated with the HCBS were found localized to nonraft microdomains. Interestingly, phosphatidylcholine (PtdCho) was selectively removed from nonraft domains by apoA-I, whereas sphingomyelin and cholesterol were desorbed from both detergent-resistant membranes and nonraft domains. The modulatory role of cholesterol on apoA-I binding to ABCA1/HCBS was also examined. Loading cells with cholesterol resulted in a drastic reduction in apoA-I binding. Conversely, depletion of membrane cholesterol by methyl-β-cyclodextrin treatment resulted in a significant increase in apoA-I binding. Finally, we obtained evidence that apoA-I interaction with ABCA1 promoted the activation and gene expression of key enzymes in the PtdCho biosynthesis pathway. Taken together, these results provide strong evidence that the partitioning of ABCA1/HCBS to nonraft domains plays a pivotal role in the selective desorption of PtdCho molecules by apoA-I, allowing an optimal environment for cholesterol release and regeneration of the PtdCho-containing HCBS. This process may have important implications in preventing and treating atherosclerotic cardiovascular disease.**—Iatan, I., D. Bailey, I. Ruel, A. Hafiane, S. Campbell, L. Krimbou, and J. Genest. **Membrane microdomains modulate oligomeric ABCA1 function: impact on apoAI-mediated lipid removal and phosphatidylcholine biosynthesis. *J. Lipid Res.* 2011.** 52: **2043–2055.**

Supplementary key words lipid and lipoprotein metabolism • high-capacity binding site • PtdCho-rich microdomains • rafts • HDL formation

Factors affecting cellular cholesterol homeostasis play a pivotal role in preventing the accumulation of excess cholesterol. Cellular cholesterol accumulation is believed to be cytotoxic to many cell types, and it is thought to contribute to foam cell death and lesional necrosis in advanced atherosclerotic cardiovascular disease (ACVD) as documented by Feng and Tabas et al. (1, 2). A substantial body of evidence from studies conducted in vitro and in vivo have shown that the ABCA1 transporter orchestrates cellular phospholipid and cholesterol removal to lipid-poor apolipoprotein acceptors by an active process. The loss of ABCA1 function in humans leads to Tangier disease, which is associated with severe HDL deficiency and increased risk of ACVD (3).

It is well accepted that apoA-I interaction with ABCA1 has important implications in the reverse cholesterol transport (RCT) process. This pathway is not only a mode of excess cholesterol removal from peripheral cells that are unable to catabolize cholesterol, including macrophages in the vessel wall, but also it is crucial for the optimal lipidation of newly synthesized apoA-I within hepatic cells in a process called nascent HDL biogenesis (4, 5). The pioneering studies by Rothblat's and Phillips' groups (6, 7) have proposed that the initial transfer of cholesterol from peripheral cells to HDL occurs via a number of

This work was supported by the Canadian Institutes of Health Research (CIHR) Grant MOP 15042 and by the Heart and Stroke Foundation of Quebec. J. Genest holds the McGill University-Novartis Chair in Cardiology.

Manuscript received 18 June 2011 and in revised form 11 August 2011.

Published, JLR Papers in Press, August 16, 2011
DOI 10.1194/jlr.M016196

Abbreviations: ACVD, atherosclerotic cardiovascular disease; CCT, CTP:phosphocholine cytidylyltransferase; CDP-cho, cytidine diphosphate choline; CDX, methyl-β-cyclodextrin; Cho, choline; CK, choline kinase; CPT, CDP-choline:DAG choline-phosphotransferase; 9CRA, 9-*cis*-retinoic acid; 2D-PAGGE, two-dimensional polyacrylamide nondenaturing gradient gel electrophoresis; DRM, detergent-resistant membrane; DSP, dithiobis(succinimidylpropionate); FC, free cholesterol; HCBS, high-capacity binding site; ICC, intracellular compartment; LpA-I, apoA-I-containing particle; 22OH, 22-(R)-hydroxycholesterol; Pcho, phosphocholine; PL, phospholipid; PM, plasma membrane; PtdCho, phosphatidylcholine; RCT, reverse cholesterol transport; TD, Tangier disease.

[1] I. Iatan and D. Bailey contributed equally to this work.
[2] To whom correspondence should be addressed.
e-mail: jacques.genest@muhc.mcgill.ca

[S] The online version of this article (available at http://www.jlr.org) contains supplementary data in the form of four figures.

mechanisms, including the aqueous diffusional/bidirectional exchange of lipids between the cell membrane and phospholipid-containing acceptors. This process has been shown to be accelerated when scavenger receptor class-B type I (SR-BI) is present (7). In contrast, cholesterol and phospholipid efflux mediated by ABCA1 transporter is unidirectional, and the primary acceptors of this pathway are lipid-poor apolipoproteins (8–10). Other ABC transporters, such as ABCG1 and ABCG4, have been shown to mediate cholesterol efflux to mature HDL particles (8).

Several models of ABCA1-mediated cholesterol efflux have been proposed, including a two-step model in which ABCA1 acts by flipping phospholipids to the outer leaflet of the plasma membrane (PM) bilayer. Subsequently, apoA-I is proposed to bind to these translocated phospholipid molecules, followed by acquisition of cholesterol and membrane solubilization (4, 6, 7). This concept is strongly supported by recent studies from our laboratory and Phillips' (9–12), in which we identified an ABCA1-dependent, phosphatidylcholine-rich, PM apoA-I binding site having a near 10-fold higher capacity to bind apoA-I compared with ABCA1. As such, we have called this site the "high-capacity binding site" (HCBS) required for apoA-I lipidation.

There is an increasing interest in understanding the role of lipid-protein interactions within specialized membrane microdomains in vascular biology and atherogenesis. Indeed, sphingolipid/cholesterol-rich rafts, known to be implicated in signal transduction, intracellular trafficking of lipids and proteins, and translocation of solutes across the membrane, have been shown to be involved in nitric oxide regulation and the RCT process (13). Earlier studies by Fielding et al. (14) have documented that PM caveolae represent a major site of efflux of both newly synthesized and low density lipoprotein-derived free cholesterol (FC) in the cells. More recently, Storey et al. (15) demonstrated selective cholesterol dynamics between lipoproteins and caveolae/lipid rafts.

Although Mendez et al. (16) have shown that membrane lipid domains distinct from cholesterol-rich rafts are involved in the ABCA1-mediated lipid secretory pathway, the nature and specifics of apoAI–ABCA1 interactions with membrane microdomains and their impact on excess cholesterol removal remain poorly understood. In this report, we examined the distribution of ABCA1 and the HCBS between membrane microdomains, explored the modulatory role of the lipid environment on ABCA1 function, and examined the potential role of apoA-I in the regulation of the phosphatidylcholine (PtdCho) biosynthesis pathway.

EXPERIMENTAL PROCEDURES

Cell culture

Human skin fibroblasts were obtained from 3.0 mm punch biopsies of the forearms of patients and healthy control subjects. Fibroblasts obtained from patients with Tangier disease (TD; homozygous for Q597R at the ABCA1 gene) were used as a negative control throughout the study as previously described (9, 17). Cells were cultured in DMEM supplemented with 0.1% nonessential amino acids, penicillin (100 U/ml), streptomycin (100 μg/ml), and 10% FBS. THP-1 macrophages were cultured under standard conditions (ATCC) and treated with 150 nM PMA for 72 h prior to use. When indicated, cells were stimulated with 2.5 μg/ml 22-(R)-hydroxycholesterol (22OH) and 10 μm 9-*cis*-retinoic acid (9CRA) for 20 h to induce ABCA1 expression. BHK cells stably transfected with an ABCA1 expression vector that is inducible by treating the cells with mifepristone and cells transfected with the same vector lacking the ABCA1 cDNA insert (mock-transfected) were generously provided by the late Dr. John F. Oram from the Department of Medicine, University of Washington, and were characterized and cultured as described previously (18). These BHK cells do not normally express ABCA1.

Human plasma apoA-I

Purified plasma apoA-I (Biodesign) was resolubilized in 4M guanidine-HCl and dialyzed extensively against PBS buffer. Freshly resolubilized apoA-I was iodinated with ^{125}Iodine by IODO-GEN® (Pierce) to a specific activity of 3,000 to 3,500 cpm/ng apoA-I and used within 48 h.

Sucrose gradient fractionation

Sucrose density gradient was performed as described previously (19). Cells were lysed at 4°C with TNE buffer [50 mM Tris-HCl (pH 7.5), 140 mM NaCl, 5 mM EDTA] containing 0.2% (v/v) Triton X-100 and protease inhibitor cocktail (Roche) for 30 min on ice followed by low-speed centrifugation to remove insoluble materials. Samples were mixed with an equal volume of 90% (w/v) sucrose in MBS [25 mM MES (pH 6.5), 150 mM NaCl] and overlaid with 35, 30, 25, and 5% (w/v) sucrose. The gradient was spun at 198,000 *g* (average) in a Beckman SW41 rotor for 16 h. Ten fractions of 1.0 ml were collected from the top and analyzed for protein, radioactivity, and lipid content.

Quantitative chemical cross-linking and immunoprecipitation assay

Quantitative immunoprecipitation was performed as we have described previously (9). Briefly, fibroblasts or PMA-treated THP-1 were incubated with 10 μg/ml of [^{125}I]apoA-I, washed with PBS, and cross-linked with 500 μM dithiobis-(succinimidylpropionate) (DSP) (Pierce) for 30min/RT. The cross-linker was inactivated by the addition of 20 mM Tris (pH 7.5) (final concentration). Cells were washed with PBS, lysed at 4°C with TNE-0.2% Triton X-100 buffer containing protease inhibitor cocktail, and subjected to sucrose fractionation. [^{125}I]apoA-I associated with ABCA1 in sucrose gradient fractions was coimmunoprecipitated with 10 μl of anti-ABCA1 antibody (Novus) for 18 h at 4°C, followed by the addition of protein A bound to Sepharose (30 μl). Radioactivity found in pellets (ABCA1-associated) and in supernatants (ABCA1-nonassociated, HCBS) was determined by γ-counting. Protein concentration was determined by standard assay (Bio-Rad).

Lipid labeling and efflux

Lipid labeling and efflux were performed as described previously (9, 20, 21) with minor modifications. Briefly, fibroblasts were labeled with either 15 μCi/ml [^{3}H]choline (Perkin-Elmer) for 48 h or 3 μCi/ml [^{3}H]cholesterol (Perkin-Elmer) for 24 h, and then stimulated as described above. Cells were subsequently incubated with lipid-free apoA-I and fractionated by sucrose gradient in the presence of 0.2% Triton X-100. For each fraction, lipids were extracted by Folch and [^{3}H]choline-labeled PtdCho, and SM were separated by TLC. [^{3}H]cholesterol was quantified directly. Alternatively, for experiments investigating the lipid composition of nascent apoA-I-containing (LpA-I) particles,

fibroblasts were labeled with 300 μCi/ml [^{32}P]orthophosphate or 15 μCi/ml [^{14}C]cholesterol, stimulated, and then incubated with lipid-free apoA-I. LpA-I particles were analyzed by two-dimensional polyacrylamide nondenaturing gradient gel electrophoresis (2D-PAGGE) and autoradiography.

Cholesterol depletion and loading

For cholesterol depletion, cells were incubated for 30 min at 37°C in DMEM containing 50 mM HEPES (pH 7.2) and 0.2% BSA (DMEM/BSA) and the indicated concentration of methyl-β-cyclodextrin (CDX). Control cells were incubated in the same medium lacking cyclodextrin. Cells were loaded with cholesterol using the above media containing the indicated concentration of the water-soluble cholesterol-cyclodextrin complex for 45 min.

Cellular [^{125}I]apoA-I binding assay

22OH/9CRA-stimulated cells were incubated with 10 μg/ml of ^{125}I-apoA-I or with increasing concentrations of ^{125}I-apoA-I for 45min at 37°C. For nonspecific binding determination, cells were incubated with a 30-fold excess of unlabeled apoA-I. ABCA1 mutant (Q597R) associated with TD was used as a negative control for binding specificity. This mutant did not show significant [^{125}I] apoA-I association with cells as we have previously described (9). After washing to remove unbound [^{125}I]apoA-I, cells were lysed in 0.1 N NaOH, and the radioactivity was determined by γ counting.

Cell surface biotinylation assay

Confluent fibroblasts were stimulated with 2.5 μg/ml 22OH and 10 μm 9CRA for 20 h. Cells were depleted of or loaded with cholesterol as described above, and then incubated with 10 μg/ml [^{125}I]apoA-I for 45 min at 37°C. Cells were washed three times with PBS, and surface proteins were biotinylated with 0.5 mg/ml sulfosuccinimidobiotin (sulfo-NHS-biotin; Pierce) for 30 min at 4°C. The biotinylation reaction was quenched by removal of the biotin solution and addition of 20 mm Tris-HCl (pH 7.5). Cells were washed twice with ice-cold PBS, lysed, and homogenized. One hundred micrograms of protein was added to 50 μl of streptavidin-Sepharose beads and incubated overnight on a platform mixer at 4°C. The PM pellet or intracellular compartment (ICC) supernatant was washed with lysis buffer. Localization of ABCA1 was monitored by Western blot and [^{125}I]apoA-I by γ counting. Results are representative of two independent experiments.

Dissociation of [^{125}I]apoA-I from intact cells

The dissociation of apoA-I was performed as we previously described (12, 20). Stimulated fibroblasts were incubated with 10 μg/ml of [^{125}I]apoA-I for 45 min at 37°C. After washing to remove unbound [^{125}I]apoA-I, DMEM was added, and the plates were immediately incubated at 37°C or 4°C for the indicated time. At each time point, the medium was replaced with fresh medium. Dissociated [^{125}I]apoA-I was determined by γ-counting. LpA-I particles were analyzed by 2D-PAGGE and autoradiography.

Analysis of gene expression by RT-PCR

Total RNA was prepared from fibroblasts and THP-1 cells using the RNeasy mini RNA extraction kit (Qiagen), according to the manufacturer's instructions. Total RNA (200 ng) was reverse-transcribed using the QuantiTect Reverse Transcription kit (Qiagen). Real-time quantitative PCR was carried out using the Quantitect SYBR Green PCR kit and QuantiTect Primer assays (Qiagen): PCYT1A (#QT00051835), PCYT1B (#QT00023380), CHKA1 (#QT00013405), and CHKB1 (#QT00218435). All reactions were performed on an ABI PRISM 7300 Sequence Detection System (Applied Biosystems). Amplifications were carried out in a 96-well plate with 50 μl reaction volumes and 40 amplification cycles (94°C, 15s; 55°C, 30s; 72°C, 34s). Experiments were carried out in triplicate, and the mRNA expression was taken as the mean of three separate experiments. The expression of each gene was normalized to glyceraldehyde-3-phosphate dehydrogenase (GAPDH) expression. Fold changes relative to controls were determined using the ΔΔCt method.

Analysis of labeled choline metabolites

The analysis of the incorporation of [^{3}H]choline into phosphocholine (Pcho), cytidine diphosphate choline (CDP-cho), and PtdCho were performed as described previously (22). Stimulated cells were incubated or not with 20 μg/ml apoA-I for 16 hr at 37°C. Cells were then pulsed with 10 μCi/ml methyl[^{3}H]choline for 1 h. After labeling, cells were washed with PBS and methanol was added. Cells were harvested by scraping and were sonicated on ice. To extract lipids, chloroform was added to the methanol-cell suspension for 15 min/RT (1:1 v/v). Water was added to separate the aqueous and lipid phases (6:6:5 methanol/chloroform/water, v/v/v). The aqueous and lipidic phases were transferred to new tubes and dried under nitrogen gas. Water-soluble metabolites were dissolved in 40 μl ethanol/water (1:1), spotted onto Whatman K5 Silica Gel Adsorption Plates (Whatman), and developed in methanol/0.9%NaCl/ammonia (50:50:5, v/v/v). Lipids were dissolved in 40 μl chloroform/methanol (2:1), spotted onto Whatman K5 Silica Gel Adsorption Plates (Whatman), and developed in chloroform/methanol/acetic acid/water (75:45:3:1, v/v/v/v). Choline, Pcho, CDP-cho, and PtdCho were identified by comigration with standards. Spots corresponding to each metabolite were revealed by iodine vapor, scraped, and then the radioactivity was determined.

Lipid and lipoproteins analysis

Cellular free and esterified cholesterol mass, as well as PtdCho were quantified by TLC. ApoA-I-containing particles were separated by 2D-PAGGE as we have previously described (23, 24).

Statistical analysis

Results were compared statistically by paired *t*-test. Two-tailed *P* values < 0.05 were considered significantly different.

RESULTS

Localization of ABCA1- and HCBS-associated apoA-I to nonraft fractions

Using detergent extraction with 0.2% Triton X-100 followed by sucrose equilibrium density gradient, we examined the localization of ABCA1, ABCA1-associated apoA-I, and HCBS-associated apoA-I to detergent-resistant membranes (DRM) and/or nonraft fractions. We chose to use 0.2% instead of 1% Triton X-100 because the latter is known to produce artifacts in the distribution of phospholipids and cholesterol between DRMs and nonraft domains, as reported by Gaus et al. (19). To ascertain the integrity of the DRMs and nonraft domains, the sucrose fractions were separated by SDS-PAGGE and monitored by appropriate antibodies for the colocalization of specific PM markers. As shown in **Fig. 1A**, extraction with 0.2% Triton X-100 followed by sucrose fractionation enabled clear separation of the DRM (raft) marker proteins caveolin-1

and flotillin-1 (fractions 1-5) from the detergent-soluble/nonraft marker transferrin receptor (TfR; fractions 6-10), as reported previously (19). As shown in supplementary Fig. I-A, ABCA1 complexes were localized exclusively to nonraft fractions (fractions 7-10). We found that ABCA1 migrated primarily in monomeric (~250 kDa) and dimeric (~500 KDa) forms, as we have documented previously (17). DTT reduced the dimeric forms to monomeric ABCA1.

Next, we examined whether the HCBS was located along with ABCA1 complexes within nonraft fractions. Fibroblasts or THP-1 cells were treated or not with 22OH/9CRA and incubated with 10 μg/ml of [^{125}I]apoA-I for 45 min at 37°C. After washing to remove unbound [^{125}I]apoA-I, cross-linking with DSP was performed and the samples were subjected to sucrose fractionation. The efficiency of DSP cross-linking was verified by cross-linking [^{125}I]transferrin to the transferrin receptor, as we have reported previously (9). To quantify the amount of HCBS- or ABCA1-associated [^{125}I]apoA-I present in each fraction, [^{125}I]apoA-I/ABCA1 complexes were directly immunoprecipitated from sucrose fractions with an anti-ABCA1 antibody, as we have reported previously (9). In both fibroblasts and THP-1, [^{125}I]apoA-I was distributed between two densities, an intermediate density (fractions 5-7) and a high density (fractions 8-10) (Fig. 1B, E). Fractions 9 and 10

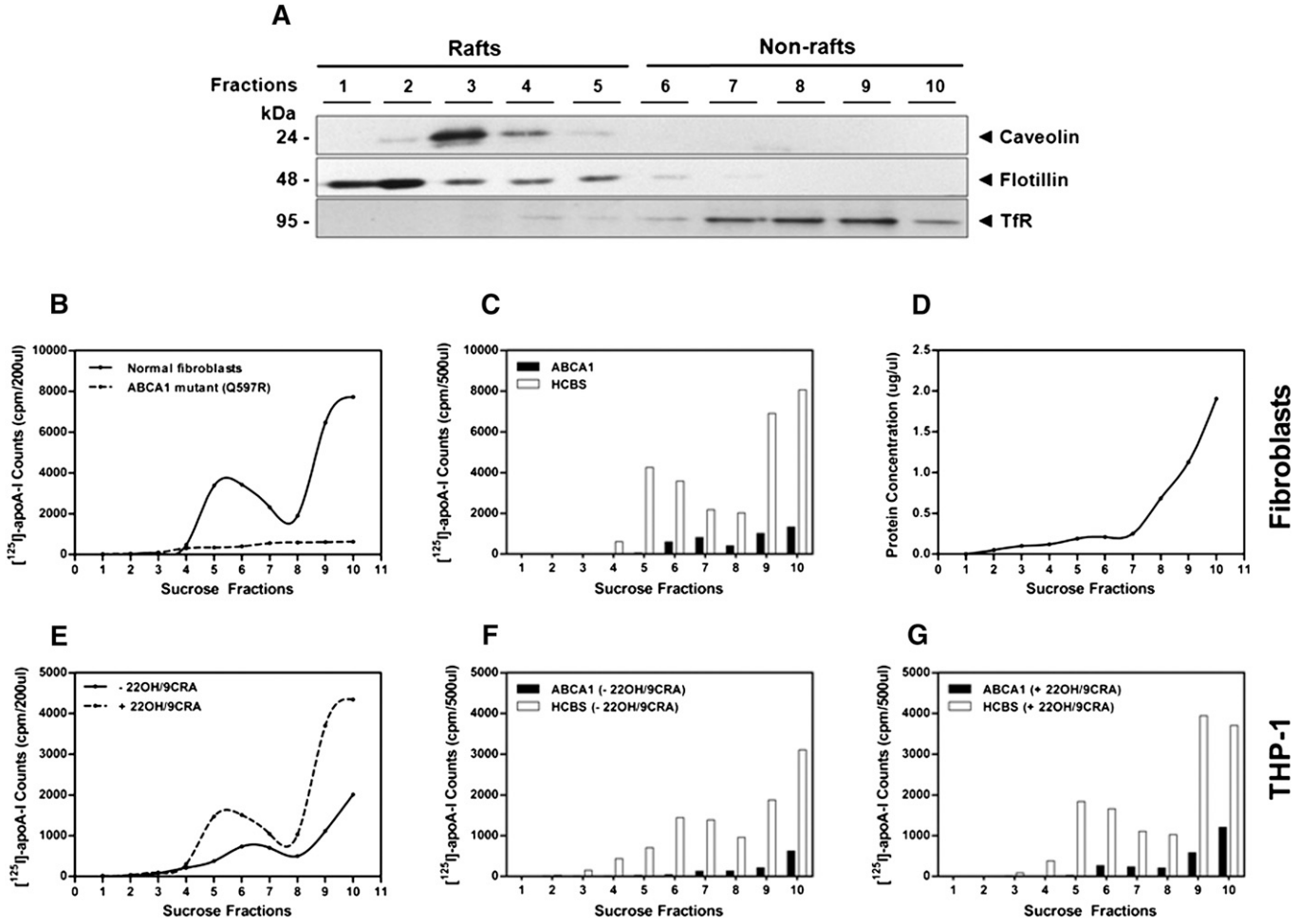

Fig. 1. Localization of ABCA1- and HCBS-associated apoA-I to nonraft fractions. (A) Normal human fibroblasts were stimulated with 22OH/9CRA for 18 h and lysed at 4°C with 0.2% Triton X-100 in TNE buffer, followed by low-speed centrifugation to remove insoluble material. Supernatants were then subjected to sucrose gradient as described in Experimental Procedures, and 10 fractions of 1 ml collected. Fractions were concentrated and subsequently separated by 4-22.5% SDS-PAGE. After electrophoresis, rafts and nonraft distribution was detected with anti-caveolin and anti-flotillin antibodies protein markers for detergent insoluble membranes and with an anti-transferrin receptor antibody for nonraft membranes. Normal and ABCA1 mutant (Q597R) human fibroblasts (B–D) and THP-1 cells (E–G) stimulated or not with 22OH/9CRA were incubated with 10 μg/ml [^{125}I]apoA-I for 45 min at 37°C. After washing to remove unbound [^{125}I]apoA-I, cross-linking with DSP was performed as described in Experimental Procedures. Cells were lysed at 4°C with 0.2% Triton X-100 in TNE buffer for 30 min followed by low-speed centrifugation to remove insoluble material. Supernatants were then subjected to sucrose gradient as described in Experimental Procedures, 10 fractions of 1 ml were collected, and radioactivity found in all fractions was determined by γ-counting. Cell associated [^{125}I]apoA-I profiles following gradient separation are shown for fibroblasts (B) and THP-1 cells (E). Fractions were subsequently concentrated and immunoprecipitated with 10 μl of affinity-purified polyclonal human anti-ABCA1 antibody (Novus) as described in Experimental Procedures. Radioactivity found in pellets (ABCA1-associated) and in supernatants (ABCA1-nonassociated, HCBS) was determined by γ-counting in fibroblasts (C), unstimulated THP-1 cells (F), and stimulated (G) THP-1 cells. Protein concentrations were assessed in fraction samples from fibroblasts (D). Results shown are representative of four independent experiments.

may potentially contain some apoA-I dissociated in vitro. Similar results were obtained using BHK cells stably overexpressing ABCA1 and HepG2 (data not shown). An ABCA1 mutant (Q597R) used as a negative control for binding specificity did not show significant [^{125}I]apoA-I association with any sucrose fraction (Fig. 1B). When [^{125}I]apoA-I was coimmunoprecipitated by an ABCA1-antibody, less than 10% of [^{125}I]apoA-I was found associated with ABCA1, whereas ~90% was found associated with the HCBS (Fig. 1C, F, G), consistent with our previous analysis of apoA-I distribution between ABCA1 and the HCBS (9, 12). Furthermore, [^{125}I]apoA-I associated with ABCA1 was localized exclusively to nonraft domains, whereas [^{125}I]apoA-I associated with the HCBS was found to partition between two densities, an intermediate density (fractions 5-7) and a high density (fractions 8-10) in both fibroblasts and THP-1 (Fig. 1B, C, E, F). A significant proportion of HCBS-associated [^{125}I]apoA-I was found associated with fractions 5 and 6, without any detectable ABCA1 as assessed by SDS-PAGGE (supplementary Fig. I-A, B). Upregulation of ABCA1 with 22OH/9CRA in THP-1 increased the association of [^{125}I]apoA-I with both ABCA1 and the HCBS in the nonraft fractions, including the less dense fractions (5–7) (Fig. 1F, G). The partition of HCBS-associated [^{125}I]apoA-I between fractions 5-7 and 8-10, the absence of ABCA1 in fraction 5 and 6, and poor protein content (Fig. 1D) suggest that the HCBS is heterogeneous in nature. We speculate that the HCBS region that excludes ABCA1 may represent exovesiculated domains or "mushroom-like protrusions" as reported by the groups of Phillips and Oram (10, 25).

ApoA-I desorbs PtdCho selectively from the HCBS within nonraft domains

We have previously reported that disruption of the HCBS by PtdCho-PLC treatment impaired apoA-I-mediated cholesterol efflux (9). The finding that the majority of apoA-I associated with the cell was found localized to the HCBS within nonraft domains (Fig. 1) suggests that apoA-I may efficiently mediate PtdCho desorption from these domains. To further examine the involvement of the HCBS in apoA-I-mediated PtdCho removal, fibroblasts were labeled with [^{3}H]choline or [^{3}H]cholesterol, stimulated with 22OH/9CRA, and incubated in the presence or absence of 15 μg/ml apoA-I for 12 h. After incubation, cells were homogenized with 0.2% Triton X-100 and subjected to sucrose fractionation. Lipids were extracted, and PtdCho and SM were quantitated by TLC. Approximately 36% of the cell content of PtdCho and 22% of SM, respectively, was found within nonraft domains, associated with the HCBS (**Fig. 2A, B**). Incubation with ApoA-I was found to promote PtdCho desorption from nonraft domains but not from DRMs (Fig. 2A). Conversely, SM and cholesterol were found to be desorbed from both nonraft domains and DRMs as shown by profiles distribution (Fig. 2B, C). This is consistent with quantification of radioactivity appearing in DRM (1 to 5) and nonraft (6 to 10) fractions expressed as percentage of control (100% in the absence of ApoA-I) for [^{3}H]PtdCho (Fig. 2D), [^{3}H]SM (Fig. 2E), and [^{3}H]cholesterol (Fig. 2F) between DRMs and nonrafts in the absence or presence of apoA-I.

On the basis of this result, we can assume that the rate of desorption of PtdCho from the HCBS is equivalent to the release of PtdCho to the media in the presence of apoA-I. As shown in supplementary Fig. II-A, apoA-I removes PtdCho from the HCBS within nonraft domains with an estimated K_m of 2 ± 0.35 μg/ml, which is characteristic of a high affinity process. These results indicate that the partitioning of ABCA1/HCBS to nonraft domains, as well as specific structural characteristics of these lipid microdomains, dictates the selective desorption of PtdCho from HCBS.

Influence of the lipid environment on the interaction of apoA-I with the ABCA1/HCBS system

The localization of ABCA1/HCBS to nonraft domains raises the possibility that the lipid constituents of the plasma membrane, namely, PtdCho and cholesterol, could be important modulators of apoA-I binding.

Given that PtdCho is a major component of the HCBS, we examined whether modulation of the PtdCho content of the cell would affect the apoA-I/HCBS interaction. To test this, we used CHO-MT58 cells, a cell line with a temperature-sensitive deficiency in CTP:phosphocholine cytidylyltransferase (CCT)α, the rate-limiting enzyme in the PtdCho biosynthesis pathway (26). At 33°C, these cells contain levels of PtdCho lower than control cells; however, they are viable and grow at an almost normal rate (27). At 40°C, however, CCTα is nonfunctional, causing a reduction in the cellular PtdCho content. CHO-MT58 and CHO-K1 cells were stimulated with T09/9CRA to induce ABCA1 expression, and then incubated with 10 μg/ml [^{125}I]apoA-I for 45 min at either permissive or restrictive temperatures. Consistent with previous analyses, at 40°C, the PtdCho content of CHO-MT58 was reduced by ~30% compared with control CHO-K1 (data not shown) (27). As shown in supplementary Fig. III-A, this reduction in PtdCho levels corresponded with a significant reduction in cellular-associated [^{125}I]apoA-I (62.6 ± 5.3% versus control). Similar ABCA1 levels were found in both cell lines at 33°C and 40°C (supplementary Fig. III-B). This result supports the role of PtdCho in associating apoA-I within the HCBS microdomains.

Additionally, we hypothesized that cholesterol may influence the association of apoA-I with the ABCA1/HCBS within nonraft domains. To examine whether membrane cholesterol is involved in the binding of apoA-I to ABCA1 and the HCBS, cells were either loaded with water-soluble cholesterol or depleted of cholesterol by incubation with CDX, and then the cellular association of [^{125}I]apoA-I was determined. Conditions were chosen so that ABCA1 levels were maintained across treatments. Loading of stimulated fibroblasts with increasing concentrations of water-soluble cholesterol significantly decreased the association of [^{125}I]apoA-I with the cells (**Fig. 3A**). Treatment with 150 μM water-soluble cholesterol increased the cellular FC content to 150 ± 6% relative to control, but it did not alter ABCA1 levels (Fig. 3B) or cause significant cellular toxicity

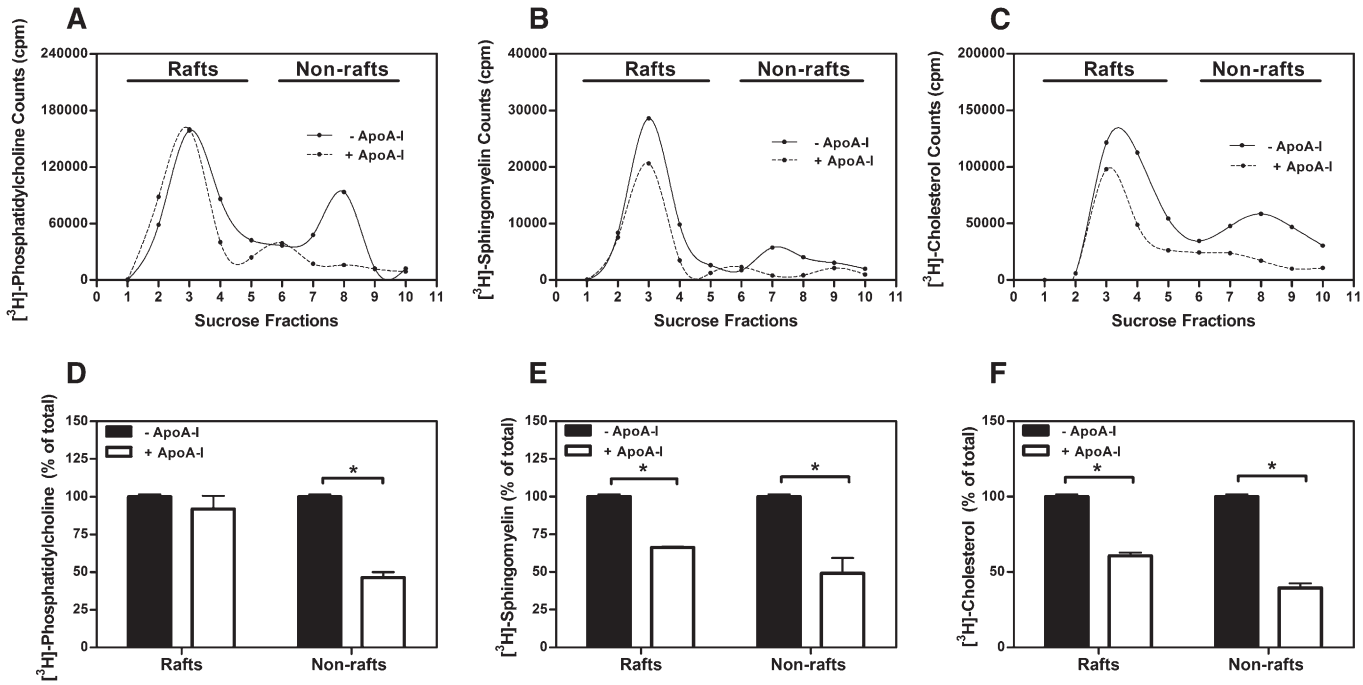

Fig. 2. ApoA-I desorbs PtdCho selectively from nonraft domains. Normal human fibroblasts were labeled with [^{3}H]choline or [^{3}H]cholesterol for 48 h, followed by stimulation with 22OH/9CRA for 18 h. Cells were incubated or not with 15 μg/ml apoA-I for 12 h and lysed at 4°C with 0.2% Triton X-100 in TNE buffer for 30 min, and then supernatants were subjected to sucrose gradient as described in Fig. 1. After lipid extraction, [^{3}H]PtdCho and [^{3}H]SM distribution in sucrose gradient fractions were assessed by TLC (A and B, respectively). [^{3}H]cholesterol (C) in each fraction was directly assessed for radioactivity. Radioactivity appearing in fractions corresponding to raft (1-5) and nonraft (6-10) material was pooled, and the desorption of [^{3}H]PtdCho (D), [^{3}H]SM (E), and [^{3}H]cholesterol (F) from raft versus nonraft in the presence of apoA-I was expressed as a percentage of control (100%, in the absence of apoA-I). Results shown are representative of three independent experiments. *$P < 0.05$ by Student's *t*-test.

as measured by an LDH-release assay (data not shown). To examine the influence of cholesterol loading on apoA-I-binding properties, stimulated fibroblasts were loaded with 150 μM cholesterol for 45 min, and then incubated with increasing concentrations of [^{125}I]apoA-I for 45 min. Cholesterol loading significantly decreased the binding capacity of apoA-I to the cell compared with control cells (B_{max} = 0.39 ± 0.09 versus 1.46 ± 0.22 ng apoA-I/μg cell protein) (Fig. 3C). In contrast, the K_d was not significantly affected (K_d = 6.14 ± 3.98 versus 5.49 ± 2.47 μg apoA-I/ml, cholesterol-loaded versus control) (Fig. 3D). This specific effect of cholesterol loading on the capacity, but not the affinity, of [^{125}I]apoA-I association with the cell suggests that cholesterol may directly affect the binding of apoA-I to the HCBS, because the HCBS is largely responsible for associating [^{125}I]apoA-I (4, 9, 11). On the contrary, cholesterol depletion by CDX significantly increased [^{125}I]apoA-I cell association at a relatively low CDX concentration (2.5 mM) (Fig. 3E). Under our experimental conditions, treatment of cells with 10 mM CDX for 30 min reduced the cellular free cholesterol content to 56 ± 3% of control cells. CDX treatment did not affect the levels of ABCA1 (Fig. 3F) or induce any cellular toxicity.

Although manipulation of cholesterol levels had a profound effect on apoA-I cellular association independent of changes in ABCA1 protein expression, it was possible that these treatments could affect the subcellular distribution of ABCA1 and, consequently, apoA-I association. To examine the effect of cholesterol loading and depletion on ABCA1 localization, distribution of ABCA1 and apoA-I between the PM and ICCs was monitored by a cell-surface biotinylation assay, as we have previously described (12). After treatment with water-soluble cholesterol, CDX, or media alone, cells were incubated with [^{125}I]apoA-I for 45 min at 37°C, and cell-surface proteins were labeled with 0.5 mg/ml sulfo-NHS-biotin for 30 min at 4°C. PM proteins were separated from intracellular proteins by streptavidin pulldown, as described in Experimental Procedures. ABCA1 localization was monitored by Western blot, whereas [^{125}I]apoA-I was quantified by γ-counting. As shown in **Fig. 4A**, the reduction or increase in [^{125}I]apoA-I binding after cholesterol or CDX treatment, respectively, was largely mediated by association with the PM. Conversely, manipulation of cholesterol levels had, at most, only a modest effect on the distribution of ABCA1 between the PM and ICCs (Fig. 4B).

The PtdCho biosynthesis pathway is regulated by apoA-I/ABCA1 interaction

After we determined that apoA-I selectively removes PtdCho from the HCBS within nonraft domains, the question was raised whether this process activates the PtdCho biosynthesis pathway. To determine the particular steps in the Kennedy pathway that were activated, ABCA1-expressing cells were incubated with apoA-I for 16 h, and then pulsed with [^{3}H]choline for 1 h. The distribution of

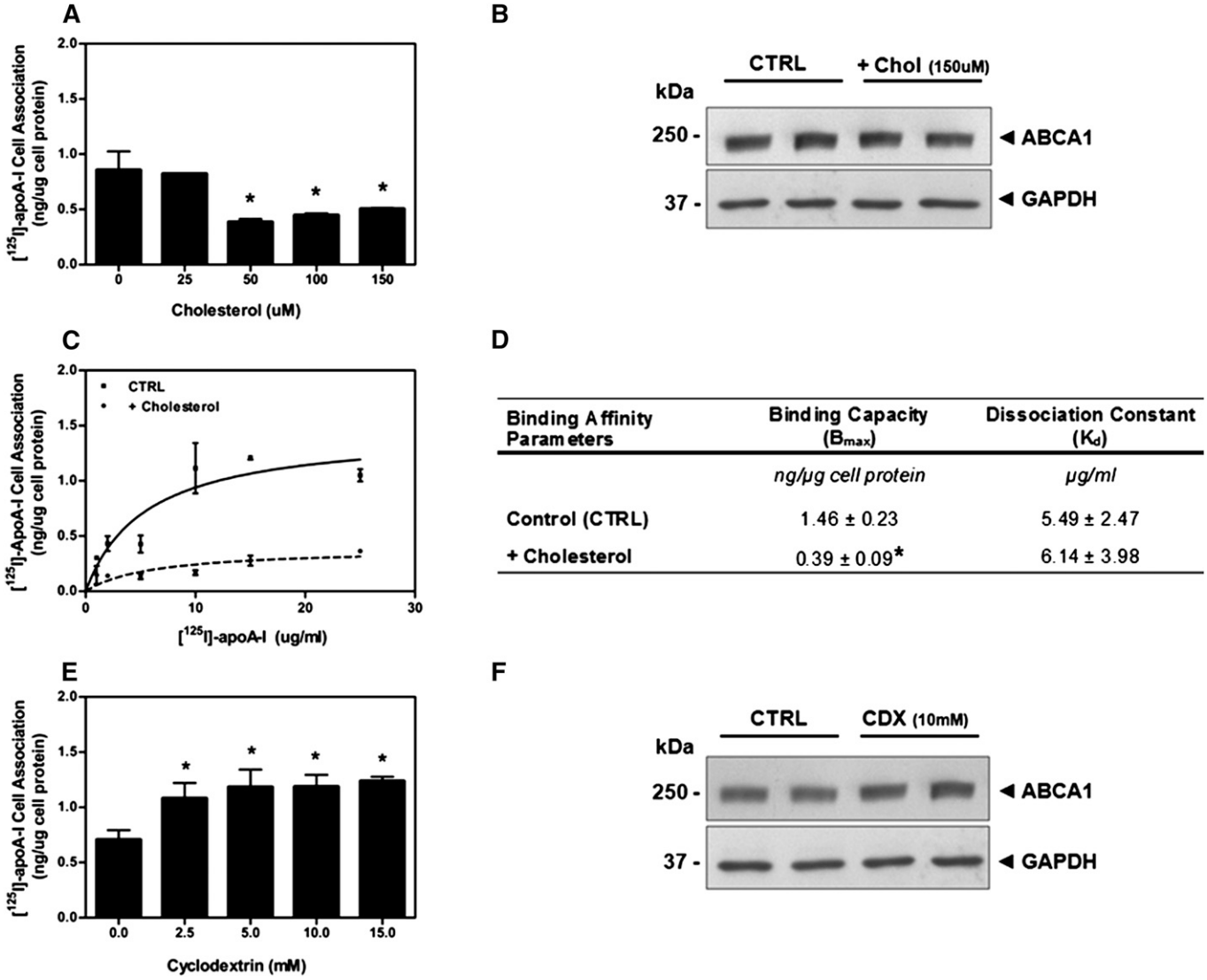

Binding Affinity Parameters	Binding Capacity (B_{max})	Dissociation Constant (K_d)
	ng/μg cell protein	*μg/ml*
Control (CTRL)	1.46 ± 0.23	5.49 ± 2.47
+ Cholesterol	0.39 ± 0.09*	6.14 ± 3.98

Fig. 3. Effect of cellular cholesterol loading and depletion on the association of apoA-I with ABCA1/HCBS. (A) Normal human fibroblasts were stimulated with 22OH/9CRA for 18 h and incubated with increasing concentrations of water-soluble cholesterol for 45 min, followed by 10 μg/ml [^{125}I]apoA-I for 45 min at 37°C. After washing to remove unbound [^{125}I]apoA-I, cells were lysed with 0.1N NaOH, and cellular associated [^{125}I]apoA-I was determined by γ-counting. Results shown are representative of three independent experiments. (B) Stimulated fibroblasts were loaded or not with 150 μM water-soluble cholesterol for 45 min, lysed, and separated by 4-22.5% SDS-PAGE. ABCA1 was detected using an affinity-purified monoclonal anti-ABCA1 antibody. GAPDH was used as a loading control. (C) Stimulated fibroblasts were loaded with 150 μM water-soluble cholesterol for 45 min and treated as in panel A. (D) Binding parameters of [^{125}I]apoA-I to both control and cholesterol-loaded samples (binding capacity B_{max} and dissociation constant K_d) were obtained using GraphPad Prism 5.0 software. Values shown are means ± SD of triplicate measures. *$P < 0.05$ by Student's *t*-test. (E) Normal human fibroblasts were stimulated with 22OH/9CRA for 18 h and incubated with increasing concentrations of CDX for 30 min. After washing, cells were incubated with 10 μg/ml of [^{125}I]apoA-I for 45 min at 37°C, washed, and lysed with 0.1N NaOH. Cellular-associated [^{125}I]ApoA-I was determined by γ-counting. Results shown are representative of three independent experiments. *$P < 0.05$ by Student's *t*-test. (F) Stimulated fibroblasts were treated or not with 10 mM CDX for 30 min, lysed, and separated by 4-22.5% SDS-PAGE. ABCA1 was detected using an affinity-purified monoclonal anti-ABCA1 antibody. GAPDH was used as a loading control.

radioactivity among the choline (Cho) metabolites [phosphocholine (Pcho), cytidine diphosphocholine (CDP-cho) and PtdCho] was quantitated by TLC after separation of the organic and aqueous phases. Incubation of 22OH/9CRA-stimulated fibroblasts with apoA-I was shown to significantly increase the incorporation of [^{3}H]choline into Pcho (∼130% versus control) and PtdCho (∼170% versus control) (**Fig. 5A**), with a concomitant depletion of [^{3}H]choline (∼30% versus control). CDP-choline did not accumulate in fibroblasts, likely because levels and/or activity of the CDP-choline:DAG choline phosphotransferase (CPT) enzyme was in excess of CCTα. Conversely, no significant increase in [^{3}H]choline conversion was observed in TD fibroblasts (Fig. 5B). Similarly, apoA-I incubation with 22OH/9CRA-stimulated THP-1 resulted in a significant increase of [^{3}H]choline incorporation into CDP-choline and PtdCho (supplementary Fig. IV-B). THP-1 incubated with 10% LPDS for 48 h was used as a positive

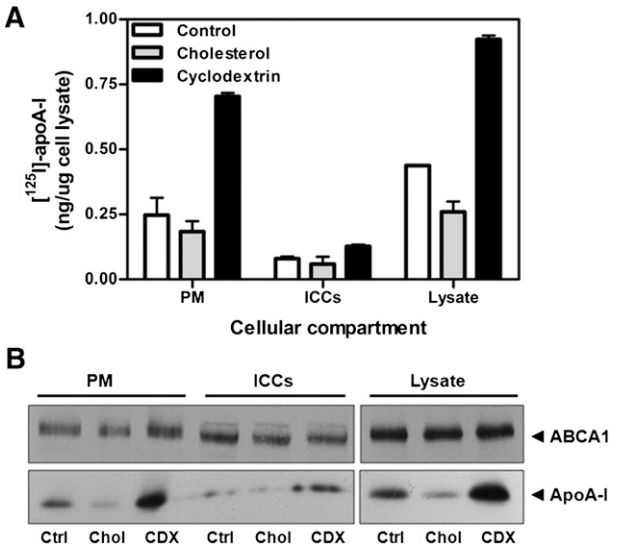

Fig. 4. ABCA1 compartmentalization under cellular cholesterol loading and depletion. (A) Confluent fibroblasts were stimulated with 2.5 μg/ml 22OH and 10 μm 9CRA for 20 h. Cells were depleted of or loaded with cholesterol as described in Experimental Procedures, and then incubated with 10 μg/ml [^{125}I]apoA-I for 45 min at 37°C. PM proteins were biotinylated with 0.5 mg/ml sulfo-NHS-biotin for 30 min at 4°C, and then separated from ICC proteins by streptavidin pulldown. [^{125}I]apoA-I was detected by γ-counting (A) and autoradiography (B), and ABCA1 was monitored by Western blot (B). Results are representative of two independent experiments.

control. Under lipoprotein deprivation incorporation of [^{3}H]choline into CDP-choline was significantly increased (data not shown), as reported previously (28).

To confirm the observation that incubation of ABCA1-expressing cells with apoA-I induces PtdCho synthesis through the Kennedy pathway, we examined the mRNA expression of CCTα, the rate-limiting enzyme in PtdCho synthesis, and choline kinase (CKα) after apoA-I incubation. As shown in Fig. 5C, incubation of apoA-I with normal fibroblasts stimulated with 22OH/9CRA induced a significant increase in mRNA expression of CCTα (2-fold versus control) and CKα (1.7-fold versus control). Incubation with apoA-I did not upregulate mRNA expression of CCTα or CKα in ABCA1 mutant (Q597R) fibroblasts (Fig. 5D). Additionally, because loss of cholesterol from the PM could stimulate PtdCho synthesis, we examined whether depletion of cholesterol with 10 mM CDX would stimulate mRNA expression of CCTα or CKα in normal fibroblasts. As shown in supplementary Fig. IV-A, CDX treatment had no significant effect on the expression of either of these genes. Incubation with apoA-I did not significantly affect gene expression from 22OH/9CRA-stimulated THP-1 cells (data not shown).

Taken together, these results suggest that ABCA1 is involved in an apoA-I-mediated upregulation of PtdCho biosynthesis. It is likely that the PtdCho depletion of the HCBS by apoA-I activates key enzymes in the PtdCho biosynthesis pathway or, alternatively, that apoA-I itself induces cell-signaling pathways that activate PtdCho synthesis directly. We are currently investigating these pathways in macrophages.

Heterogeneity of nascent LpA-I released during dissociation from HCBS

As shown in Fig. 1, after 45 min incubation at 37°C, the majority of apoA-I was found associated with the HCBS, as we have previously reported (9, 12). In an attempt to examine the nature of the nascent LpA-I particles released from the HCBS, we monitored the dissociation of the lipidated apoA-I products. [^{125}I]apoA-I was incubated with stimulated fibroblasts for 45 min at 37°C. After washing to remove unbound [^{125}I]apoA-I, the plates were incubated with DMEM alone at 37°C or 4°C for the indicated time. At each of the indicated time points, the medium was replaced with fresh medium. As shown in **Fig. 6**, [^{125}I]apoA-I dissociated from wild-type cells in two peaks (Peak I and Peak II). Dissociation of [^{125}I]apoA-I was inhibited at 4°C, suggesting that dissociation was not an artifactual release of apoA-I after extensive washing of the cells. An ABCA1 mutant (Q597R) that has been shown to have no significant apoA-I binding was used as a negative control. Analysis of the dissociated lipidated apoA-I products by 2D-PAGGE revealed initial dissociation (Peak I) generated α-LpA-I particles with sizes of 8 nm (Fig. 6B), whereas later dissociation (Peak II) produced larger α-LpA-I with sizes between 9 and 17 nm (Fig. 6E). The α-electrophoretic mobility of dissociated LpA-I was determined based on a standard reference gel depicting the preβ electrophoretic mobility of lipid-free apoA-I (Fig. 6A) (12). To assess the lipid composition of the nascent LpA-I particles, cells were loaded with [^{32}P]orthophosphate or [^{14}C]cholesterol to label the phospholipid and cholesterol components, respectively. Cells were stimulated and then incubated with lipid-free apoA-I. Collection fractions corresponding to Peaks I and II were pooled and washed extensively by filtration to remove free [^{32}P]phospholipids and [^{14}C]cholesterol. Samples were concentrated and analyzed by 2D-PAGGE and followed by autoradiography. Initial dissociation of apoA-I from the HCBS was found to produce particles containing phospholipids but no detectable cholesterol (Fig. 6C, D), whereas later dissociation was found to produce particles containing both phospholipids and cholesterol. PtdCho was a major phospholipid species found in those small particles (Peak I), as assessed by TLC (data not shown). These results suggest that apoA-I could be initially released from the HCBS as small PtdCho-apoA-I discs and that these discs may interact successively with different microdomains, including DRMs (raft), to acquire cholesterol.

DISCUSSION

The concept proposed by the Phillips and Rothblat groups that apoA-I-mediated membrane solubilization pathway efficiently clears cells of excess cholesterol has important implications in the RCT process and atherogenesis (10, 29). Defining the lipid microenvironment surrounding oligomeric ABCA1, which likely influences its conformation, function, and regulation, is key for understanding how the cholesterol homeostasis pathway and nascent HDL biogenesis are regulated at the cellular level.

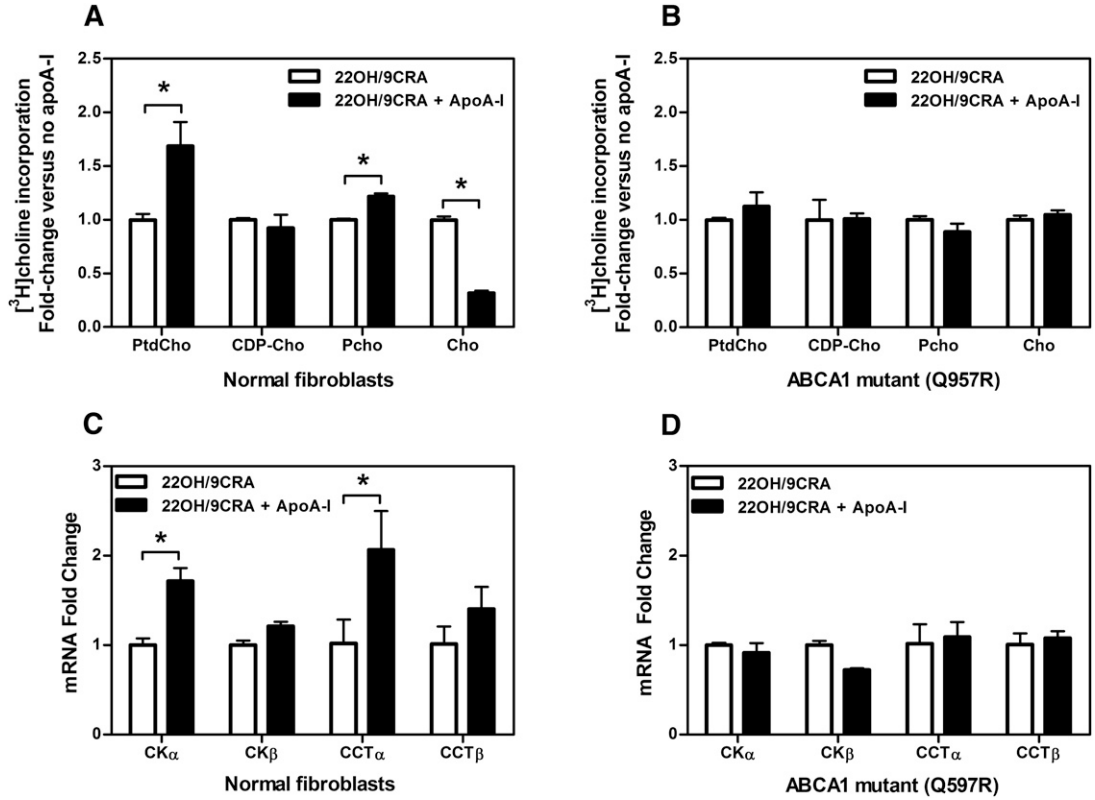

Fig. 5. The PtdCho biosynthesis pathway is regulated by apoA-I/ABCA1 interaction in fibroblasts. (A, B) Normal and ABCA1 mutant (Q597R) fibroblasts were stimulated with 22OH/9CRA and incubated or not with 20 μg/ml apoA-I for 16 h. Cells were then pulsed with 10 μCi/ml methyl[^{3}H]choline for 1 h, and the distribution of radioactivity among metabolites (Cho, Pcho, and CDP-cho) and PtdCho was determined as described in Experimental Procedures. Values shown are means ± SD of triplicate measures. *$P < 0.05$ by Student's *t*-test. (C, D) Stimulated normal and ABCA1 mutant (Q597R) fibroblasts were incubated or not with 20 μg/ml apoA-I for 16 h, followed by mRNA extraction using the RNeasy mini RNA extraction kit (Qiagen). Analysis of mRNA expression of CCTα, CCTβ, CKα, and CKβ was carried by real-time quantitative PCR from 200 ng total RNA as described in Experimental Procedures. Values shown are means ± SD of triplicate experiments. The expression of each gene was normalized to GAPDH expression, and mRNA fold changes relative to controls were determined. *$P < 0.05$ by Student's *t*-test.

Here, we obtained evidence that both ABCA1 and the HCBS were localized to nonraft domains in fibroblasts and THP-1 stimulated with 22OH/9CRA (Fig. 1 and supplementary Fig. I), consistent with our previous report documenting that ABCA1 and the HCBS were found in the Triton X-100 soluble fraction (9). The exclusion of ABCA1 and the HCBS from raft domains could be an intrinsic property of the transporter. Indeed, Landry et al. (30) have reported that, through its ATPase-related functions, ABCA1 expression alters the general packing of the PM by generating more loosely packed microdomains. This finding is in agreement with a recent study by Zarubica et al. (31) reporting that analysis of the partitioning of dedicated probes in PM-vesiculated blebs allowed visualization of ABCA1 partitioning into the liquid disordered-like phase and corroborated the idea that ABCA1 destabilizes the lipid arrangement at the PM. Their finding supports the concept that ABCA1 plays a pivotal role in controlling transversal and lateral lipid distribution at the PM and positions the effluxes of cholesterol from the cell membrane to the redistribution of the sterol into readily extractable membrane pools.

An earlier study from our laboratory (17) proposed that a homotetrameric complex of ABCA1 constitutes the minimal functional unit required for apoA-I lipidation, in agreement with the work done by the Chimini group (32). It is possible that generation of the HCBS stabilizes ABCA1 clustering, which can influence both the initial association of apoA-I to ABCA1 and the ABCA1 oligomerization state, thereby maximizing the number of apoA-I molecules that bind to the oligomeric ABCA1 simultaneously. This is consistent with the finding that apoA-I binds to tetrameric and dimeric, but not monomeric, forms of ABCA1 (17).

The phospholipid translocase activity of ABCA1 appears to create two populations of HCBS microdomains within the nonraft fractions that could impact both the capacity of the membrane to associate with apoA-I and the composition of the nascent HDL products. We obtained evidence that the HCBS is heterogeneous, based on the observation that apoA-I was distributed between two physically distinct density regions (Fig. 1). In the intermediate density fractions, ABCA1 was absent, whereas in the higher density fractions, ABCA1 was present, as were the majority of membrane proteins (supplementary Fig. I). It is likely that the HCBS associated with the less dense intermediate fractions, which are relatively rich in lipids and poor in membrane proteins (Fig. 1D), represent the "mushroom-like

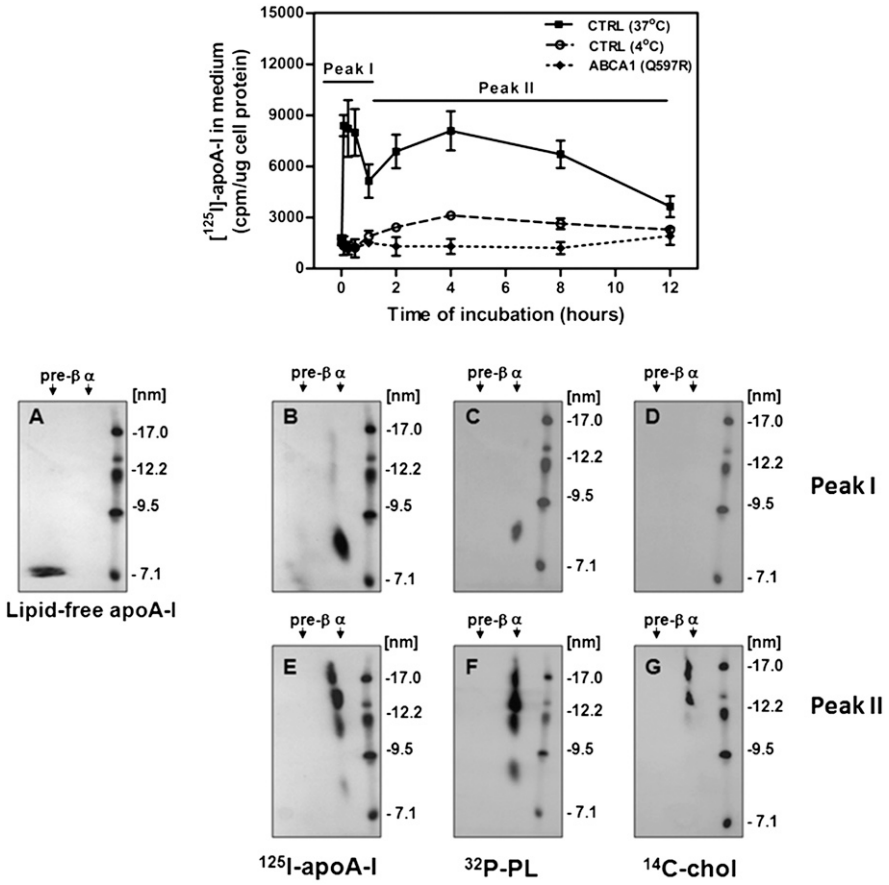

Fig. 6. Heterogeneity of nascent LpA-I released during dissociation from HCBS. (Top) Normal and ABCA1 mutant (Q597R) fibroblasts were stimulated with 22OH/9CRA and incubated in the presence of 10 μg/ml of [^{125}I]apoA-I for 45 min at 37°C. After washing to remove unbound [^{125}I]apoAI, DMEM was added, and plates were immediately incubated at 37°C or 4°C. Medium was removed and replaced with fresh medium for the indicated time period. Dissociated [^{125}I]apoA-I was determined by γ-counting. (Bottom) Analysis of the dissociated lipidated apoA-I products by 2D-PAGGE. The α-electrophoretic mobility of dissociated LpA-I was determined based on a standard reference gel depicting the preβ electrophoretic mobility of lipid-free apoA-I (A) (12). To assess the lipid composition of the nascent LpA-I particles, fibroblasts were incubated with 300 μCi of [^{32}P]orthophosphate for 72 h (C, F) or with 15 μCi/ml of [^{14}C]cholesterol for 24 h (D, G). Cells were stimulated with 22OH/9CRA and incubated with lipid-free apoA-I under similar conditions as described above. Released ApoA-I particles pertaining to each peak were pooled, concentrated, and analyzed for lipid content on 2D-PAGGE as described in Experimental Procedures. The presence of [^{125}I] apoA-I, [^{32}P]phospholipids, or [^{14}C]cholesterol was detected by autoradiography.

protrusions" or exovesiculated domains to which apoA-I binds on the surface of human fibroblasts and THP-1, as reported by Lin and Oram (25). This is in line with the idea of Vedhachalam et al. (11) that "plasma membrane proteins (including ABCA1) are presumably excluded from the exovesiculated domains" and that these domains are formed from regions of protein-free PM that are likely to be relatively fluid.

The structural and physicochemical characteristics that dictate the partitioning of ABCA1 and apoA-I to nonraft domains are presently unknown. We obtained evidence to support the role of PtdCho in apoA-I association (Fig. 5 and supplementary Fig. III) (9); however, the peaks of PM levels of PtdCho separated by sucrose fractionation do not appear to correlate directly with the peaks of apoA-I binding (Fig. 1 versus Fig. 2A). We hypothesize that the cholesterol composition of membrane microdomains could play a major role in partitioning both ABCA1/HCBS and apoA-I to nonraft domains. It is possible that the greater lipid lateral packing density within cholesterol-rich raft domains could reduce the affinity of apoA-I to these microdomains. Here, we obtained evidence to support this concept. First, we demonstrate that cholesterol loading of cells, without altering ABCA1 levels, drastically reduced the binding of apoA-I to ABCA1/HCBS (Fig. 3A–D). Second, depletion of cholesterol from cells using a low concentration of CDX, which is known to disrupt rafts, significantly increased the association of apoA-I to ABCA1/HCBS, without significantly changing ABCA1 levels (Fig. 3E, F). It is possible that excess cholesterol directly affects the conformation of the oligomeric ABCA1 or the packing of PtdCho molecules within the HCBS populations, and thereby reduces the affinity for apoA-I. These results are supported by studies using artificial membranes showing

that apoA-I efficiently solubilizes multilamellar vesicles of the loosely packed L_d phase (33). Alternatively, cholesterol could directly modulate the activity of ABCA1. This idea is supported by a previous study by Ueda's group documenting that the ATPase activity of purified ABCA1 in PtdCho-liposomes was significantly decreased by enrichment with cholesterol (34). The disturbance of ABCA1/HCBS system by excess cholesterol accumulation within foam cells may have a direct impact on the development of atherosclerotic lesions. Indeed, Choi et al. (35) have recently documented that accumulation of cholesterol by intimal arterial smooth muscle cells (SMC) resulted in the impairment of both apoA-I-mediated cholesterol efflux and apoA-I binding to the cells.

Previous studies from our laboratory and others have not supported the existence of a clear precursor-product relationship between the various nascent LpA-I particles (20, 36, 37). In this report, by monitoring the dissociation of apoA-I from the HCBS, we observed the production of, initially, small LpA-I particles with a high phospholipid-to-cholesterol ratio, and subsequently, larger LpA-I particles containing both phospholipids and cholesterol (Fig. 6). These results are consistent with findings by Mulya and Sorci-Thomas et al. (38, 39). The smaller particles could represent initial PtdCho-apoA-I discs that arise from the HCBS and interact successively with different microdomains, including rafts, to acquire cholesterol and produce the larger particles. Indeed, we observed that apoA-I selectively desorbs PtdCho from HCBS within nonraft domains and cholesterol from DRMs (Fig. 2). This finding is in agreement with a previous study by Mendez et al. (16), showing that membrane lipid domains distinct from cholesterol/SM rich rafts are involved in the lipidation of apoA-I, whereas membrane rafts are involved in efflux to lipidated particles. Additionally, small HDL particles enriched in phospholipids but depleted of cholesterol have been shown to be one of the most efficient acceptors of cellular cholesterol (40). Alternatively, the complexity of the larger particles could require a longer incubation period for production. This idea is in agreement with a previous study by the Jessup group demonstrating that two kinetically distinguishable pathways of cholesterol transfer to apoA-I exist (41), as well as a study by the Parks laboratory demonstrating that larger nascent particles are produced only with prolonged apoA-I incubation (42). In this case, the heterogeneity of the LpA-I particles may reflect simultaneous microsolubilization of lipids from distinct microdomains, consistent with our observation that apoA-I associated with the HCBS was found in two physically distinct densities (Fig. 1) that likely reflect heterogeneity in membrane lipid composition. This hypothesis is in accordance with the microsolubilization mechanism supported by Vedhachalam et al. (10).

The interaction of apoA-I with the ABCA1/HCBS system was found to significantly increase PtdCho synthesis (Fig. 5). Indeed, we obtained evidence that both CKα and CCTα gene expression were significantly upregulated following incubation of the cell with apoA-I. This is in agreement with an earlier study by Mallampalli's group (28) that documented that lipoprotein deprivation upregulates the gene expression and activity of CCTα in alveolar type II epithelial cell line. Furthermore, Shiratori et al. (43) have reported that FC loading of macrophages upregulates CCTα activity by a posttranslational mechanism and that the increased of PtdCho biosynthesis is an adaptive response to accommodate the excess cholesterol. The activation of the PtdCho biosynthetic pathway by apoA-I may be physiologically important in the regeneration of the HCBS, allowing the removal of excess cholesterol from PM microdomains. Whether apoA-I directly induces a cell-signaling pathway that stimulates PtdCho biosynthesis or it activates PtdCho production via an adaptive response to PtdCho depletion is currently under investigation.

As summarized in **Fig. 7**, our current working model of apoA-I lipidation is as follows. The lipid translocase activity of oligomeric ABCA1 creates a heterogenous HCBS population, including the exovesiculated HCBS that excludes ABCA1 and the HCBS that associates with oligomeric ABCA1 complexes. Initial interactions of apoA-I with the oligomeric ABCA1 facilitate its translocation to the HCBS populations from which apoA-I desorbs PtdCho, becoming an efficient acceptor of cholesterol. These small PtdCho-containing particles may interact successively or simultaneously with different microdomains, including cholesterol-rich rafts, allowing the formation of larger, heterogeneous, cholesterol-containing nascent LpA-I particles. The desorption of PtdCho molecules by apoA-I induces an adaptive response to upregulate the PtdCho biosynthesis pathway, thereby allowing replenishment of the lost membrane PtdCho and regeneration of HCBS populations. The model presented in Fig. 7 is a simple illustration of our current findings and previous investigations on the ABCA1/HCBS system (4, 9–12). Our findings are in agreement with the model proposed recently by Phillips' group (11) in which the initial event consists of the binding of a small pool of apoA-I to ABCA1 at the PM, stimulating the net phospholipid translocation to the exofacial leaflet. This situation leads to unequal lateral packing densities in the two leaflets of the phospholipid bilayer, creating exovesiculated lipid domains. The formation of a highly curved membrane surface promotes high affinity binding of apoA-I to these domains. This pool of bound apoA-I spontaneously solubilizes the exovesiculated domain to create discoidal nascent HDL particles. The identification and isolation of HCBS populations as reported here (Fig. 1) will certainly aid the analysis of the lipidome of these domains and the determination of their impact on the assembly of nascent particles, their composition, and speciation. The detailed mechanisms underlying apoA-I interactions with membrane microdomains require more extensive investigations, which are currently ongoing.

The present report provides a biochemical basis for apoA-I-mediated plasma microdomain excess cholesterol removal that involves both the oligomeric ABCA1 and the HCBS population. This process may have important implications in preventing and treating atherosclerotic cardiovascular disease.

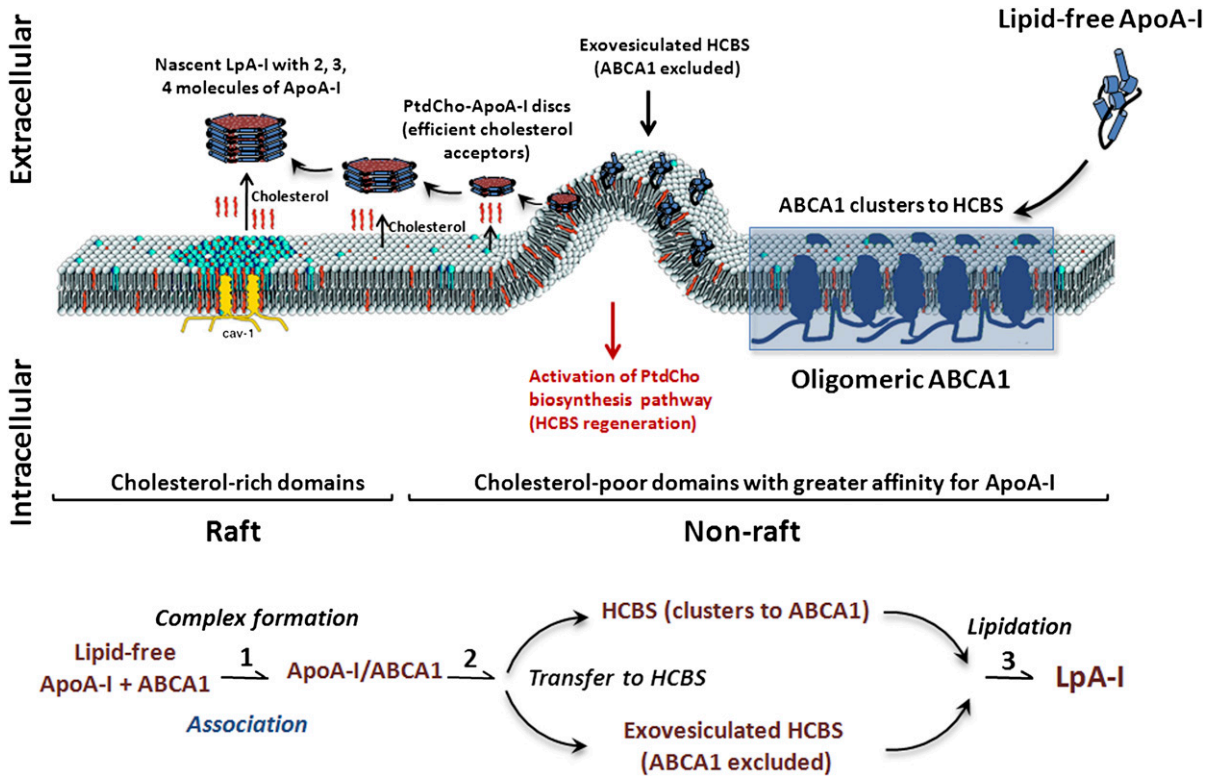

Fig. 7. A proposed model for apoA-I interaction with ABCA1 within PM microdomains. Lipid free apoA-I initially interacts with oligomeric ABCA1 through a rapid but transient association. The phospholipid translocase activity of ABCA1 creates heterogenous HCBS microdomain populations within the nonrafts composed of an ABCA1-excluded exovesiculated HCBS domain and a HCBS that clusters with oligomeric ABCA1 complexes. ABCA1 subsequently mediates the transfer of apoA-I to these HCBS populations, from which apoA-I selectively desorbs PtdCho to become PtdCho-apoA-I discs. Subsequently, apoA-I obtains PtdCho and cholesterol to generate heterogenous nascent LpA-I particles with two, three, and four molecules of apoA-I. The desorption of PtdCho by apoA-I activates the PtdCho biosynthesis pathway, thereby allowing replenishment of the lost membrane PtdCho and regeneration of the HCBS populations.

The authors express their gratitude to the late Dr. John F. Oram and to Dr. Ashley M. Vaughan for generously providing BHK cells overexpressing ABCA1 and to Dr. Dennis Vance for kindly providing CHO-MT58 cells. The authors are grateful for Tudor Iatan's assistance in editing the proposed model.

REFERENCES

1. Feng, B., P. M. Yao, Y. Li, C. M. Devlin, D. Zhang, H. P. Harding, M. Sweeney, J. X. Rong, G. Kuriakose, E. A. Fisher, et al. 2003. The endoplasmic reticulum is the site of cholesterol-induced cytotoxicity in macrophages. *Nat. Cell Biol.* **5:** 781–792.
2. Tabas, I. 2002. Consequences of cellular cholesterol accumulation: basic concepts and physiological implications. *J. Clin. Invest.* **110:** 905–911.
3. Brooks-Wilson, A., M. Marcil, S. M. Clee, L-H. Zhang, K. Roomp, M. van Dam, L. Yu, C. Brewer, J. A. Collins, H. O. F. Molhuizen, et al. 1999. Mutations in *ABC1* in Tangier disease and familial high-density lipoprotein deficiency. *Nat. Genet.* **22:** 336–345.
4. Krimbou, L., M. Marcil, and J. Genest. 2006. New insights into the biogenesis of human high-density lipoproteins. *Curr. Opin. Lipidol.* **17:** 258–267.
5. Lee, J. Y., and J. S. Parks. 2005. ATP-binding cassette transporter AI and its role in HDL formation. *Curr. Opin. Lipidol.* **16:** 19–25.
6. Rothblat, G. H., F. H. Mahlberg, W. J. Johnson, and M. C. Phillips. 1992. Apolipoproteins, membrane cholesterol domains, and the regulation of cholesterol efflux. *J. Lipid Res.* **33:** 1091–1097.
7. Yancey, P. G., A. E. Bortnick, G. Kellner-Weibel, M. de la Llera-Moya, M. C. Phillips, and G. H. Rothblat. 2003. Importance of different pathways of cellular cholesterol efflux. *Arterioscler. Thromb. Vasc. Biol.* **23:** 712–719.
8. Cavelier, C., I. Lorenzi, L. Rohrer, and A. von Eckardstein. 2006. Lipid efflux by the ATP-binding cassette transporters ABCA1 and ABCG1. *Biochim. Biophys. Acta.* **1761:** 655–666.
9. Hassan, H. H., M. Denis, D. Y. Lee, I. Iatan, D. Nyholt, I. Ruel, L. Krimbou, and J. Genest. 2007. Identification of an ABCA1-dependent phospholipid-rich plasma membrane apolipoprotein A-I binding site for nascent HDL formation: implications for current models of HDL biogenesis. *J. Lipid Res.* **48:** 2428–2442.
10. Vedhachalam, C., P. T. Duong, M. Nickel, D. Nguyen, P. Dhanasekaran, H. Saito, G. H. Rothblat, S. Lund-Katz, and M. C. Phillips. 2007. Mechanism of ATP-binding cassette transporter A1-mediated cellular lipid efflux to apolipoprotein A-I and formation of high density lipoprotein particles. *J. Biol. Chem.* **282:** 25123–25130.
11. Vedhachalam, C., A. B. Ghering, W. S. Davidson, S. Lund-Katz, G. H. Rothblat, and M. C. Phillips. 2007. ABCA1-induced cell surface binding sites for apoA-I. *Arterioscler. Thromb. Vasc. Biol.* **27:** 1603–1609.
12. Hassan, H. H., D. Bailey, D. Y. Lee, I. Iatan, A. Hafiane, I. Ruel, L. Krimbou, and J. Genest. 2008. Quantitative analysis of ABCA1-dependent compartmentalization and trafficking of apolipoprotein A-I: implications for determining cellular kinetics of nascent high density lipoprotein biogenesis. *J. Biol. Chem.* **283:** 11164–11175.
13. Mason, R. P., and R. F. Jacob. 2003. Membrane microdomains and vascular biology: emerging role in atherogenesis. *Circulation.* **107:** 2270–2273.
14. Fielding, P. E., and C. J. Fielding. 1995. Plasma membrane caveolae mediate the efflux of cellular free cholesterol. *Biochemistry.* **34:** 14288–14292.
15. Storey, S. M., A. M. Gallegos, B. P. Atshaves, A. L. McIntosh, G. G. Martin, R. D. Parr, K. K. Landrock, A. B. Kier, J. M. Ball, and F. Schroeder. 2007. Selective cholesterol dynamics between lipoproteins and caveolae/lipid rafts. *Biochemistry.* **46:** 13891–13906.
16. Mendez, A. J., G. Lin, D. P. Wade, R. M. Lawn, and J. F. Oram. 2001. Membrane lipid domains distinct from cholesterol/

sphingomyelin-rich rafts are involved in the ABCA1-mediated lipid secretory pathway. *J. Biol. Chem.* **276:** 3158–3166.
17. Denis, M., B. Haidar, M. Marcil, M. Bouvier, L. Krimbou, and J. Genest. 2004. Characterization of oligomeric human ATP binding cassette transporter A1. Potential implications for determining the structure of nascent high density lipoprotein particles. *J. Biol. Chem.* **279:** 41529–41536.
18. Oram, J. F., A. M. Vaughan, and R. Stocker. 2001. ATP-binding cassette transporter A1 mediates cellular secretion of alpha-tocopherol. *J. Biol. Chem.* **276:** 39898–39902.
19. Gaus, K., M. Rodriguez, K. R. Ruberu, I. Gelissen, T. M. Sloane, L. Kritharides, and W. Jessup. 2005. Domain-specific lipid distribution in macrophage plasma membranes. *J. Lipid Res.* **46:** 1526–1538.
20. Denis, M., B. Haidar, M. Marcil, M. Bouvier, L. Krimbou, and J. Genest, Jr. 2004. Molecular and cellular physiology of apolipoprotein A-I lipidation by the ATP-binding cassette transporter A1 (ABCA1). *J. Biol. Chem.* **279:** 7384–7394.
21. Krimbou, L., M. Denis, B. Haidar, M. Carrier, M. Marcil, and J. Genest, Jr. 2004. Molecular interactions between apoE and ABCA1: impact on apoE lipidation. *J. Lipid Res.* **45:** 839–848.
22. Gasull, T., E. Sarri, N. DeGregorio-Rocasolano, and R. Trullas. 2003. NMDA receptor overactivation inhibits phospholipid synthesis by decreasing choline-ethanolamine phosphotransferase activity. *J. Neurosci.* **23:** 4100–4107.
23. Krimbou, L., M. Tremblay, J. Davignon, and J. S. Cohn. 1997. Characterization of human plasma apolipoprotein E-containing lipoproteins in the high density lipoprotein size range: focus on pre-beta1-LpE, pre-beta2-LpE, and alpha-LpE. *J. Lipid Res.* **38:** 35–48.
24. Bailey, D., I. Ruel, A. Hafiane, H. Cochrane, I. Iatan, M. Jauhiainen, C. Ehnholm, L. Krimbou, and J. Genest. 2010. Analysis of lipid transfer activity between model nascent HDL particles and plasma lipoproteins: implications for current concepts of nascent HDL maturation and genesis. *J. Lipid Res.* **51:** 785–797.
25. Lin, G., and J. F. Oram. 2000. Apolipoprotein binding to protruding membrane domains during removal of excess cellular cholesterol. *Atherosclerosis.* **149:** 359–370.
26. Vance, D. E., C. J. Walkey, and Z. Cui. 1997. Phosphatidylethanolamine N-methyltransferase from liver. *Biochim. Biophys. Acta.* **1348:** 142–150.
27. Lee, M. W., M. Bakovic, and D. E. Vance. 1996. Overexpression of phosphatidylethanolamine N-methyltransferase 2 in CHO-K1 cells does not attenuate the activity of the CDP-choline pathway for phosphatidylcholine biosynthesis. *Biochem. J.* **320:** 905–910.
28. Ryan, A. J., D. M. McCoy, S. N. Mathur, F. J. Field, and R. K. Mallampalli. 2000. Lipoprotein deprivation stimulates transcription of the CTP:phosphocholine cytidylyltransferase gene. *J. Lipid Res.* **41:** 1268–1277.
29. Gillotte, K. L., M. Zaiou, S. Lund-Katz, G. M. Anantharamaiah, P. Holvoet, A. Dhoest, M. N. Palgunachari, J. P. Segrest, K. H. Weisgraber, G. H. Rothblat, et al. 1999. Apolipoprotein-mediated plasma membrane microsolubilization. Role of lipid affinity and membrane penetration in the efflux of cellular cholesterol and phospholipid. *J. Biol. Chem.* **274:** 2021–2028.
30. Landry, Y. D., M. Denis, S. Nandi, S. Bell, A. M. Vaughan, and X. Zha. 2006. ATP-binding cassette transporter A1 expression disrupts raft membrane microdomains through its ATPase-related functions. *J. Biol. Chem.* **281:** 36091–36101.
31. Zarubica, A., A. P. Plazzo, M. Stockl, T. Trombik, Y. Hamon, P. Muller, T. Pomorski, A. Herrmann, and G. Chimini. 2009. Functional implications of the influence of ABCA1 on lipid microenvironment at the plasma membrane: a biophysical study. *FASEB J.* **23:** 1775–1785.
32. Trompier, D., M. Alibert, S. Davanture, Y. Hamon, M. Pierres, and G. Chimini. 2006. Transition from dimers to higher oligomeric forms occurs during the ATPase cycle of the ABCA1 transporter. *J. Biol. Chem.* **281:** 20283–20290.
33. Fukuda, M., M. Nakano, S. Sriwongsitanont, M. Ueno, Y. Kuroda, and T. Handa. 2007. Spontaneous reconstitution of discoidal HDL from sphingomyelin-containing model membranes by apolipoprotein A-I. *J. Lipid Res.* **48:** 882–889.
34. Takahashi, K., Y. Kimura, N. Kioka, M. Matsuo, and K. Ueda. 2006. Purification and ATPase activity of human ABCA1. *J. Biol. Chem.* **281:** 10760–10768.
35. Choi, H. Y., M. Rahmani, B. W. Wong, S. Allahverdian, B. M. McManus, J. G. Pickering, T. Chan, and G. A. Francis. 2009. ATP-binding cassette transporter A1 expression and apolipoprotein A-I binding are impaired in intima-type arterial smooth muscle cells. *Circulation.* **119:** 3223–3231.
36. Krimbou, L., H. Hajj Hassan, S. Blain, S. Rashid, M. Denis, M. Marcil, and J. Genest. 2005. Biogenesis and speciation of nascent apoA-I-containing particles in various cell lines. *J. Lipid Res.* **46:** 1668–1677.
37. Liu, L., A. E. Bortnick, M. Nickel, P. Dhanasekaran, P. V. Subbaiah, S. Lund-Katz, G. H. Rothblat, and M. C. Phillips. 2003. Effects of apolipoprotein A-I on ATP-binding cassette transporter A1-mediated efflux of macrophage phospholipid and cholesterol: formation of nascent high density lipoprotein particles. *J. Biol. Chem.* **278:** 42976–42984.
38. Mulya, A., J. Y. Lee, A. K. Gebre, M. J. Thomas, P. L. Colvin, and J. S. Parks. 2007. Minimal lipidation of pre-beta HDL by ABCA1 results in reduced ability to interact with ABCA1. *Arterioscler. Thromb. Vasc. Biol.* **27:** 1828–1836.
39. Sorci-Thomas, M. G., J. S. Owen, B. Fulp, S. Bhat, D. Shah, G. W. Jerome, M. Zabalawi, and M. J. Thomas. 2011. Composition of nascent HDL by ABCA1: lipidomics for efficient cholesterol packaging and particle production (Abstract in Arteriosclerosis, Thrombosis, and Vascular Biology, 2011 Scientific Sessions. Chicago, IL, April 28-30, 2011).
40. Castro, G. R., and C. J. Fielding. 1988. Early incorporation of cell-derived cholesterol into pre-beta-migrating high-density lipoprotein. *Biochemistry.* **27:** 25–29.
41. Gaus, K., J. J. Gooding, R. T. Dean, L. Kritharides, and W. Jessup. 2001. A kinetic model to evaluate cholesterol efflux from THP-1 macrophages to apolipoprotein A-1. *Biochemistry.* **40:** 9363–9373.
42. Mulya, A., J-Y. Lee, A. K. Gebre, E. Y. Boudyguina, S-K. Chung, T. L. Smith, P. L. Colvin, X-C. Jiang, and J. S. Parks. 2008. Initial interaction of apoA-I with ABCA1 impacts in vivo metabolic fate of nascent HDL. *J. Lipid Res.* **49:** 2390–2401.
43. Shiratori, Y., A. K. Okwu, and I. Tabas. 1994. Free cholesterol loading of macrophages stimulates phosphatidylcholine biosynthesis and up-regulation of CTP: phosphocholine cytidylyltransferase. *J. Biol. Chem.* **269:** 11337–11348.